Reelin Is Involved in the Crypt-Villus Unit Homeostasis

Pablo García-Miranda, Ph.D.,[1] María D. Vázquez-Carretero, Ph.D.,[1] Pilar Sesma, Ph.D.,[2] María J. Peral, Ph.D.,[1] and Anunciación A. Ilundain, Ph.D.[1]

[1]Department of Physiology; Faculty of Pharmacy, University of Seville, Seville, Spain.
[2]Department of Histology and Pathological Anatomy, Faculty of Biology, University of Navarra, Pamplona, Spain.

Intestinal myofibroblasts secrete substances that control organogenesis and wound repair of the intestine. The myofibroblasts of the rat small intestine express reelin and the present work explores whether reelin regulates crypt–villus unit homeostasis using normal mice and mice with the reelin gene disrupted (reeler). The results reveal that mouse small intestine expresses reelin, its receptors apolipoprotein E receptor 2 (ApoER2) and very low-density lipoprotein receptor (VldlR) and the reelin effector protein Disabled-1 (Dab1) and that reelin ex- pression is restricted to myofibroblasts. The absence of reelin significantly reduces epithelial cell proliferation, migration, and apoptosis and the number of Paneth cells. These effects are observed during the suckling, weaning, and adult periods. The number of Goblet cells is increased in the 2-month-old reeler mice. The absence of reelin also expands the extracellular space of the adherens junctions and desmosomes without significantly affecting either the tight-junction structure or the epithelial paracellular permeability. In conclusion, this is the first *in vivo* work showing that the absence of reelin alters intestinal epithelium homeostasis.

Introduction

THE EPITHELIUM of the mammalian gastrointestinal tract has the most rapid turnover rate of any tissue in the body and its homeostasis requires carefully choreographed programs of cell proliferation, growth arrest, migration/ differentiation, and apoptosis. In rodents, the epithelium of the small intestine is completely replaced every 2–3 days. Cell proliferation is confined to the crypts of Lieberkü hn, where the stem cells give rise to progenitor cells, which are amplified by constant division along the bottom two thirds of the crypts. Cell cycle arrests and differentiation occurs when cell progenitors reach the crypt–villus junction, and the villus constitutes the differentiated and functional compart ment.

Absorptive enterocytes,hormone-secreting enteroendocrine cells, opioid-producing brush (tuff) cells, microfold (M) cells, and mucus-producing Goblet cells emerge from the crypts and complete their differentiation as they migrate up the adjacent villi in vertical coherent columns.[1] When mature cells approach the apical extrusion zone of the villus they suffer apoptosis and are exfoliated into the gut lumen,[2] thus balancing the continuous produc- tion of new cells. The antibacterial peptide-secreting Paneth cells also arise from the multipotent crypt stem cell, but they migrate toward the crypt base, where they survive for around 6–8 weeks before being eliminated by phagocytosis.[3]

Spontaneous apoptosis in the crypts is rare and it may serve to remove defective/injured progeny cells and senescent Paneth cells.[4]

Epithelial cell renewal is strictly controlled by cell–cell and cell–extracellular matrix (ECM) interactions.[5] A thin and continuous sheet of ECM, the basement membrane (BM), separates epithelial cells from the interstitial connective tis- sue and its composition defines the necessary microenvironment required for multiple cellular functions during development and at maturity. Reciprocal interactions be- tween the epithelium and the underlying BM regulate proliferation, migration, differentiation, apoptosis, morpho- genesis, tissue repair, inflammation, and the immune re- sponse.[6] Numerous receptors for ECM molecules have been identified in the intestinal epithelial cells, many of which are integrins.[7] However the nature of cell–BM interactions and their intracellular processing remains largely undefined. Within the ECM, the myofibroblasts, located beneath the epithelia, express and secrete various ECM components, such as cytokines, growth factors, chemokines, hormones, neurotransmitters, inflammatory mediators, and adhesion proteins, as well as express receptors for many of these ligands, allowing information flow in both directions, to and from the

intestinal epithelium and the ECM.[6,8] As a consequence, the myofibroblasts are regarded as a cell that orchestrates functions that ranged from control of epithelial renewal processes to peripheral immune tolerance.[6,8]

We reported that: (1) the mucosa of rat small intestine expresses reelin, its receptors apolipoprotein E receptor 2 (ApoER2) and the very low-density lipoprotein receptor (VldlR), and its effector protein Disabled-1 (Dab1) and (2) within the intestinal mucosa, reelin expression was restricted to myofibroblasts.[9] In brain, the reelin secreted by the Cajal– Retzius cells is critical for the positioning of migrating neurons during the development of the central nervous system.[10] Because differentiation of the intestinal epithelial cells requires their migration along the crypt–villus axis, we reasoned that the reelin released by the myofibroblasts to the ECM might regulate epithelial dynamics.[9]

The present work explores *in vivo* whether reelin is involved in the crypt–villus unit homeostasis. For that, we have examined the consequences of reelin gene disruption on cell proliferation, migration, differentiation, and apoptosis in the epithelium of mice small intestine. A preliminary report of some of these results was published as an abstract.[11]

Methods

[^{14}C]-Polyethylene glycol-4000 ([^{14}C]-PEG-4000) was purchased from GE Healthcare. Anti-reelin antibodies were obtained from Santa Cruz Biotechnology, Inc. (sc-5578) and Calbiochem (553731); the anti-cleaved Caspase-3 (Asp175) antibody from Cell Signaling and the anti-E-Cadherin anti- body from the BD Transduction Laboratories (610181). Un- less otherwise stated, the other reagents were obtained from Sigma-Aldrich.

Animals

Reeler (rl) is a spontaneous autosomal recessive mutation.[10] Heterozygous (*rl*$^{+}$/*rl*$^{-}$) mice C57BL/6 were purchased from Jackson Laboratories through Charles River Laboratories. Control (*rl*$^{+}$/*rl*$^{+}$) and homozygous mutant reeler (*rl*$^{-}$/*rl*$^{-}$) mice were obtained by heterozygous crossings. Fifteen- and 21-day-old and 1-, 2-, 3-, and 18-month-old mice were used. The animals were housed in a 12:12 light–dark cycle and fed *ad libitum* with the Global 2019 extruded rodent diet (Harlan Ibérica S.L.) with free access to tap water. Mice were genotyped by polymerase chain reaction (PCR) analysis of genomic DNA using the primers (5¢-3¢) TAATCTGTCCTCACTCTGCC, CAGTTG ACATACCTTAAT, and TGCATTAATGTGCAGTGT.

The mice were humanely handled and sacrificed, by cervical dislocation, in accordance with the European Council legislation 86/609/EEC concerning the protection of experimental animals.

Relative quantification of real-time reverse transcription-PCR

Total RNA was extracted from the small intestine using the RNeasy® kit (Qiagen). cDNA was synthesized from 1 mg of total RNA using the QuantiTect® reverse transcription kit (Qiagen) as described by the manufacturer. Real-time reverse transcription (RT)-PCR was performed with iQ™SYBR® Green Supermix (BioRad), 0.4-mM primers, and 1 mL cDNA. Controls were carried out without cDNA. Amplification was run in a MiniOpticon™ System (BioRad) thermal cycler (94°C/3 min; 35 cycles of 94°C/40 s, 58°C/40 s and 72°C/ 40 s, and 72°C/2 min). Following amplification, a melting curve analysis was done by heating the reactions from 65°C to 95°C in 1°C intervals, while monitoring fluorescence. Analysis confirmed a single PCR product at the predicted melting temperature. Primers for the genes tested are given in Table 1. b-Actin served as the reference gene and was used for samples normalization. The cycle at which each sample crossed a fluorescence threshold (Ct) was determined and the triplicate values for each cDNA were averaged. Analyses of PCR were done using the comparative Ct method with the Gene Expression Macro software supplied by BioRad.

Isolation of enterocytes and myofibroblats

Enterocytes and mucosal myofibroblasts enriched fractions were isolated as described.[9] Briefly, the small intestine was rapidly removed and washed with an ice-cold saline solution. One centimeter intestinal segments were incubated at room temperature in the phosphate-buffered saline (PBS) buffer containing 1 mM dithiothreitol for 15 min, fol- lowed by a 30-min incubation period at 37°C in a calcium- and magnesium-free PBS buffer containing 1 mM EDTA and 2 mM glucose. Following incubation, the tissues were vor- texed for 30 s, the loosened epithelial cells (enterocytes) were filtered through 60-mm nylon textile, and collected by cen- trifugation and resuspension in PBS. For myofibroblats iso- lation, the remaining tissue was rinsed in PBS and incubated for 30 min, in a shaking water bath at 37°C, in PBS containing 1 mg mL^{-1} collagenase and 2 mg mL^{-1} hyaluronidase. The pieces were vortexed for 30 s and the myofibroblasts were pelleted and resuspended in PBS. The isolated cells were immediately used for immunostaining.

Immunostaining analysis

Enterocytes, myofibroblasts, and intact small intestine were used for immunostaining studies. Immunostaining as- says were performed on intact small intestine (either 10-mm cryosections or 5-mm paraffin sections) and on isolated intestinal cells, as previously.[9] The slides containing either the intestinal sections or the isolated cells were incubated with the indicated primary antibody at 4°C, overnight. Antibody binding was visualized with biotinylated anti IgG anti- bodies, at dilution 1:100, followed by immunoperoxidase staining. The Vectastain ABC peroxidase kit (Vector) and 3,3¢-diaminobenzidine were used for the tissue cryosections and the 3-amino-9 ethylcarbazole for paraffin sections. Controls were carried out without a primary antibody. The slides were rinsed, mounted, and photographed with a Zeiss Axioskop 40 microscope equipped with a SPOT Insight V 3.5 digital camera. Acquired images were analyzed by using Spot Advance 3.5.4.1 program (Diagnostic Instrument, Inc.).

Western assays

SDS-PAGE was performed on a 15% polyacrylamide gel as described.[12] For protein extraction, the small intestine was homogenized in a buffer containing in mM, 150 NaCl, 50 Tris/HCl, 1 EDTA, pH 7.4, 0.01 aprotinin, 0.01 leupeptin and
0.2 phenylmethylsulfonylfluoride and 1% Triton X-100. Following the 10-min incubation, the suspension was centrifuged at 14,000 *g* for 30 min. The resultant supernatant was dissolved in the Laemmli sample buffer, electrophoresed, and electrotransferred onto a nitrocellulose membrane (Micron Separations, Inc.). A total of 50 mg protein was loaded to each lane. The protein was measured by the Bradford method using gamma globulin as the standard. The immunoreactive bands were viewed using a chemiluminescence procedure (GE Healthcare). The anti-b-actin antibody (1:1000 dilution) was used to normalize band density values. The relative abundance of the bands was quantified using PCBAS program version 2.0 (Raytest).

Crypt cell proliferation rate

The epithelial cell proliferation rate was quantified by measuring the incorporation into DNA of 5-bromo deoxy- uridine (BrdU). Mice received an intraperitoneal injection of BrdU (120 mg/kg body weight) and were killed 90 min later. BrdU was detected by immunohistochemistry using a monoclonal anti-BrdU antibody, 1:300 dilution, as described above. The

number of labeled cells in 30 crypts well-oriented longitudinally per mouse was determined by light micros- copy. The crypt cell proliferation rate is expressed as the number of BrdU-positive cells per crypt.

Epithelial cell migration rate

Mice were killed 32 h after the intraperitoneal injection of BrdU (120 mg/kg). Small intestinal sections were processed for immunoperoxidase staining to detect BrdU-labeled cells as described above. The epithelial cell migration rate was estimated by measuring the distance from the base of the villus to the foremost-labeled cell at 32 h after injection. Thirty villi well-oriented longitudinally per mouse were used. The cell migration rate is expressed as mm/h.

Analysis of cell apoptosis

The identification and quantification of apoptotic cells in the epithelium of the small intestine were performed by immunological detection (Western blot and immunohistochemistry assays) of cleaved Caspase-3. A polyclonal anti- cleaved Caspase-3 antibody was used at dilution 1:1000 for the Westerns and at dilution 1:200 for immunohistochemistry. The number of labeled cells in 100 well-oriented longitudinally villi per mouse was determined by light microscopy. Results are expressed as the number of labeled cells per 10 villi.

Goblet cells staining

The identification and quantification of Goblet cells in the epithelium of the small intestine were performed using Periodic Acid-Shiff (PAS) Staining System as indicated by the manufacturer. The number of labeled cells in 30 villi well- oriented longitudinally per mouse was determined and the results are expressed as the number of Goblet cells per villus.

Paneth cells staining

Small intestine Paneth cells were quantified by phloxine- tartrazine histological stain. Briefly, 10-mm cryosections of small intestine were incubated with the hematoxylin solution (Gill No. 3) for 3 s, followed by a 2-min incubation in a 70% ethanol solution containing in mM, 6 phloxine and 34 $CaCl_2$. After being washed with tap water, they were placed in a solution containing 9.4 mM tartrazine in 2-ethoxy-ethanol for
1.5 h, and thereafter they were washed with 2-ethoxy-etha- nol. The number of labeled cells in 30 crypts well-oriented longitudinally per mouse was determined and the results are given as the number of Paneth cells per crypt.

Electron microscopy assays

Segments of small intestine were fixed in 4% glutaraldehyde/0.1 M sodium cacodylate, pH 7.4 at 4°C for 3 h. After three rinses in the cacodylate-buffered solution, the tissues were postfixed in 1% OsO_4 in 0.1 M phosphate buffer at 4°C for 1 h and washed in the cacodylate-buffered solution containing 7.5% sucrose. The segments were then dehydrated in a graduated series of acetone (30%, 50%, and 70%), stained with 2% uranyl acetate and embedded in Spurr's epoxy re- sin. Ultrathin sections were examined either under a Philips CM-10 or a Zeiss Libra 120 transmission electron micro- scopes equipped with an Olympus Veleta or a TRS 2K Slow-scam CCD camera, respectively. The photographs were processed with iTEM software.

Assessment of intestinal permeability to [^{14}C]-*PEG-4000*

Intestinal permeability to [^{14}C]-PEG-4000 was measured using everted intestinal sacs, according to Wilson and Wise- man.[13] Briefly, the small intestine was dissected, rinsed twice with ice-cold saline solution, turned inside out, and cut into two to three parts. Each part was closed at one end using a cotton thread. Each sac was filled through the other end with the modified Krebs–Ringer bicarbonate-phosphate buffer containing in mM, 140

NaCl, 10 $KHCO_3$, 3 K_2HPO_4, 1.2 $CaCl_2$, and 1.2 $MgCl_2$, pH 7.4 and closed. The sacs were incubated, at 37°C in a thermostatic bath with continuous shaking, in modified Krebs–Ringer bicarbonate-phosphate buffer, pH 7.4, containing [^{14}C]-PEG-4000 (1.2 mM), that was continuously bubbled with 95%O_2/5%CO_2. After a 5-min incubation period, the everted sacs were rinsed with the ice- cold saline solution, opened, and the serosal fluid collected. The sacs were weighed wet before and after the incubation period. Fifty microliters samples were taken from the bathing solution and from the serosal fluid for radioactivity counting. The sacs were opened longitudinally and the serosal surface area was evaluated by measuring the length and width of the open sac. The amount of [^{14}C]-PEG-4000 in the serosal side was referred to the intestinal surface area.

Statistical analysis

Data are presented as mean – SEM. Unless stated other- wise, the number of animals (*n*) used in each experimental condition was three control and three reeler mice. In the Figures, the vertical bars that represent the SEM are absent when they are less than symbol height. In Figures 1 and 9, comparisons between different experimental groups were evaluated by the two-tailed Student's *t*-test. One-way ANOVA followed by the Newman-Keuls' test was used for multiple comparisons (GraphPad Prism program). Differences were set to be significant for $p < 0.05$.

Results

Expression of reelin, Dab1, VldlR, and ApoER2 in the mice small intestine

The experiments were performed to find out whether murine small intestine expresses reelin, its effector protein Dab1, and its receptors VldlR and ApoER2. Figure 1 shows the relative abundance of reelin, Dab1, VldlR, and ApoER2 mRNAs in the intestine of control and reeler mice. As expected, the small intestine of the reeler mice lacks reelin mRNA. The mRNA levels of Dab1 and VldlR were similar in both types of mice, but the mutation significantly decreases the abundance of ApoER2 mRNA.

As myofibroblasts express a-smooth muscle actin (a- SMA), we have used the anti-a-SMA antibody to their localization in the mucosa of mice intestine. The localization of a-SMA and reelin proteins in mice intestine is shown in Figure 2. In the intestine of control mice, the specific signal produced by the anti-reelin antibody is restricted to a layer of cells located beneath the epithelium. This layer is also reactive to the anti-a-SMA antibody. In the intestine of the reeler mice, the anti-a-SMA antibody also produces a specific signal in the layer of cells located beneath the epithelium, but these cells do

not react to the anti-reelin antibody.

The observations made in isolated cells (Fig. 2) corroborate those made in intact tissue. Thus, the myofibroblasts isolated from the small intestinal mucosa of control mice present a strong reelin-specific immunostaining signal. Immunoreactive reelin signal is neither seen in the myofibroblasts of the reeler mice nor in the enterocytes of either type of mouse.

Immunoreactive signal was not seen in the absence of the corresponding primary antibody (data not shown).

These observations together, indicate that reelin is only produced by the myofibroblasts placed underneath the epithelium of mice intestine.

Cell proliferation rate in the small intestinal epithelium of control and reeler mice

To assess the effects of the reeler mutation on epithelial cell proliferation, the incorporation of BrdU into DNA was measured in the epithelium of the small intestine of control and reeler mice of different ages, as explained in the Methods section. The results are given in Figure 3. As expected, BrdU-positive nuclei are only found in the crypt cells and their quantification reveals that in control mice the cell proliferation rate increases during the 2nd month of life, and thereafter it remains fairly constant. In the reeler mice, the epithelial cell proliferation remains fairly constant during the first 2 months of life and it significantly increased thereafter.

In all the ages examined, the epithelial cell proliferation rate is around 22% – 5% lower in the reeler mice as compared with that measured in the control animals.

Cell migration rate in the small intestinal epithelium of control and reeler mice

BrdU incorporation into DNA was also used to evaluate the cell migration rate as described in the Methods section and the results are given in Figure 4. They reveal that the pattern of cell migration rate along the villi is similar in both types of mice. It peaks at 1 month of age and it remains fairly constant in the adult animal.

In all the ages tested, the cell migration rate measured in the intestinal epithelium of the reeler mice is around 37% – 5% lower compared with control mice.

Cell apoptosis in the small intestinal epithelium of control and reeler mice

Cell apoptosis was evaluated by immunological detection of cleaved Caspase-3. The immunohistochemistry assay reveals that in both, control and reeler mice, the apoptotic cells are only observed at the villi (Fig. 5). In

all the ages tested, the number of apoptotic cells in reeler mice is around 50% – 5% of that measured in the control mice.

The Westerns assays (Fig. 6) show that the anti-cleaved Caspase-3 antibody detected polypeptides of 17 and 19 kDa, being the former more abundant that the 19-kDa polypeptide. The 17-kDa polypeptide is indicative of cleaved Caspase-3[14] and the mutation significantly decreases its abundance in all the ages tested.

Number of Goblet cells in the small intestinal epithelium of control and reeler mice

Goblet cells were identified using the PAS staining system. The results are given in Figure 7 and reveal that the number of PAS-positive cells in the intestinal epithelium of the control mice peaks at 1 month of age, it decreases at 2 months, and thereafter it increases with age. In the intestine of the reeler mice, the number of Goblet cells increases from the 2nd week of life to 1 month, it remains constant during the following month, and thereafter it increased with age.

Significant differences in the number of Goblet cells be- tween the two types of mice are only observed at 2 months of age: they are lower in the control mice than in the reeler.

Number of Paneth cells in the small intestinal epithelium of control and reeler mice

We identified Paneth cells in the intestinal mucosa of control and reeler mice using phloxine-tartrazine histological stain. Figure 8 shows that in both, reeler and control mice, the number of Paneth cells increases during the first 2 months of life and it slightly decreases at 18 months.

In all the ages tested, the reeler mutation reduces the number of Paneth cells by 30% – 1.8% as compared with the values obtained in control mice.

Electron microscopy studies of the small intestine of control and reeler mice

We have investigated whether reelin affects the organization of the cell–cell junctions. The microvilli and cell–cell contacts were examined by electron microscopy (Fig. 9). It is observed that the microvilli are numerous and well formed in both types of mice. No significant differences between the control and reeler mice are found in either the length or the number of microvilli (data not shown).

The microphotographs of Figure 9 reveal that the tight junctions appear normal, but the intercellular space of both, the adherens junctions and

desmosomes is significantly wider in the reeler than in the control mice.

Immunolocalization of E-cadherin in the small intestinal epithelium of control and reeler mice

Immunohistochemical assays reveal that a strong E-cadherin- specific immunostaining signal is located at the lateral membrane of the epithelial cells, in both control and reeler mice (Fig. 10). No significant differences between the two types of mice are observed, indicating that the protein is properly located to the membrane in the intestine of both, control and reeler of mice. Immunoreactive signal was not seen in the absence of the primary antibody (data not shown).

Intestinal transport of [^{14}C]-PEG-4000 in control and reeler mice

Mucosal to serosal transfer of [^{14}C]-PEG-4000 was measured to estimate the paracellular permeability of the jejunum and ileum of control and reeler mice. Everted intestinal sacs were used and the age of the animals was 21 days old. The results reveal that the mucosal to serosal transfer of [^{14}C]-PEG-4000 is similar in both types of mice (1.48 – 0.21 and 1.16 – 0.34 pmol/cm^2 in jejunum and ileum of control mice, respectively, vs. 1.17 – 0.15 and 1.19 – 0.06 pmol/cm^2 in jejunum and ileum of reeler mice, respectively, $n = 5$).

Discussion

The myofibroblasts placed underneath the epithelium of the small intestine secrete substances that control the epithelial cell renewal as well as intestinal organogenesis and wound repair.[6] We previously proposed that in the rat small intestine the reelin released by the myofibroblasts might regulate the crypt–villus unit homeostasis[9] and the current data support this point of view. The results also show that the epithelial cell renewal processes vary with age, as previously reported for control mice,[15] and that reelin does not modify the pattern of this age-related changes.

As observed in rat,[9] expression of reelin in mice small intestine is restricted to the myofibroblasts placed under- neath the epithelium and the following data suggest that reelin regulates crypt–villus unit dynamics. The mutation decreases cell proliferation in the crypts, which suggests that reelin stimulates stem cells. The replication and division of the stem cells in the crypts force the migration of their daughters toward the villi. If reelin promotes proliferation of intestinal stem cells, differences on cell migration speed be- tween the two types of mice should occur, and indeed cell migration along the villi is significantly reduced by the reeler mutation.

Slowed migration, however, could also be secondary to increased apoptosis in the crypts: if fewer cells exited the crypt, the rate of movement up the villus would be reduced. However, apoptotic cells are only observed at the villi tip, which agrees with studies showing that apoptosis occurs predominantly at the villus tip.[16] The observations discussed so far might suggest that reelin has a growth- promoting action in the small intestine. In contradiction to this point of view is that no differences in the height of the villi between control and reeler mice were observed, though the villi width was decreased by the mutation.[17] The length of the villi is also determined by apoptosis at the villi and the absence of reelin decreases the number of apoptotic cells in the villi, but this decrease is approximately two times lower than that measured in the cell proliferation rate. The magnitude of the reelin-related changes in the crypt–villus unit cell renewal processes described here is similar to that re- ported for mice intestine in response to other experimental challenges,[18–20] but different results have been found in the literature. As in the current work, some investigators re- ported diminutions in cell proliferation and migration rates without changes in the villi height,[18,21] but others found decreases in cell proliferation and migration that were ac- companied by a smaller villi size.[22–24] It has been observed that, when they occur together, the changes in cell proliferation and migration rates go in the same direction,[18,21–24] but different situations have been described regarding apoptosis: changes in either the same direction than those found in cell proliferation,[25] in the opposite direction[26] or no change.[19–21] The current results also suggest that reelin regulates epithelial cell differentiation because its absence decreases the number of Paneth cells. The number of Goblet cells, how- ever, is either unchanged or increased in the 2-month-old reeler mice. The physiological meaning of these observations is not evident, but the different effects of the mutation on the number of Paneth and Goblet cells suggest that the two cell lineages have different requirements for their differentiation. Decreases in the number of Paneth without changes in that of Goblet cells[27] or vice versa[25] have been reported.

Adhesion junctions are vital for epithelial sheets as they maintain tissue integrity and epithelial homeostasis[28] and the reeler mutation significantly expands the extracellular space of the adherens junctions and desmosomes. The mutation does not seem to modify the tight junctions as both, its appearance at the electronic microscopy and the intestinal transport of PEG-4000, a molecule that crosses the intestinal epithelium via the paracellular route, is similar in both types of mice. The adhesive function of the adherens junctions and desmosomes is mediated by the cadherins ectodomain, which engages identical molecules on the surface of the ad- jacent cell. The

expansion of the adherens junctions does not appear to be due to mislocalization of cadherin because the mutation does not modify the cell location of the E-cadherin. The capacity of reelin to regulate cell proliferation, migration, and differentiation agrees with observations made in neural[29–31] and non-neural tissues, such as submandibular[32] and mammary gland.[33] However, inhibition of cell migration in primary cultures of mammary epithelial cells[33] and of apoptosis in embryonic carcinoma cells[34] by exogenous reelin have also been reported. Whereas the information on the cell-signaling cascades initiated by reelin in brain is profuse, the studies on the role of reelin in non-neural tissues are scarce. Due to the cross talk between myofibroblasts and epithelial cells,[6] the intestinal effects of reelin reported here could be triggered by either a direct action of reelin on the epithelial cells or through a reelin-induced change in the myofibroblasts or by both ways. Neither are known the molecular mechanism(s) by which reelin exerts these effects. We have reported that in mice small intestine, the reeler mutation modifies the expression of genes coding for proteins that control epithelial cell renewal processes and cytoskeleton organization.[17] Let us mention the mutation- induced downregulation of Arrb1 (b1-arrestin) and PyCard and the upregulation of bone morphogenetic protein 1 (Bmp1), peroxisome proliferator-activated receptor alpha (Ppara), and Eph receptor A1 (EphA1). The effects of the mutation on Bmp1, Ppara, and b1-arrestin could mediate the mutation-induced decrease in cell proliferation reported here, because: (1) Bmp1 stimulates the BMP pathway,[35] a signaling system that inhibits cell proliferation,[36] (2) Ppara inhibits cell proliferation,[37] and (3) the downregulation of b1- arrestin might reduce the activity of the Wnt system,[38] which is known to stimulate intestinal cell proliferation.[36] The Wnt system also controls the number of Paneth cells[36] and the downregulation of b1-arrestin and the mutation-induced decrease in the number of Paneth cells could be related. The minor intestinal cell migration seen in the reeler mice may, in part, result from the upregulation of the EphA1 receptor because its activation inhibits cell migration *in vitro*.[39] Finally, the decrease in cell apoptosis observed in the reeler intestine may depend on the downregulation of the proapoptotic PyCard gene.[40] Cell proliferation and migration and the structure of the apical junctions depend on the dynamics of the actin cytoskeleton. In the small intestine, b1-arrestin activates the actin-depolymerizing factor/cofilin.[41]The absence of reelin may inactivate intestinal cofilin via down-regulation of b1-arrestin and, hence, modify those cell processes that depend on the actin cytoskeleton. Although in the brain, reelin inactivates cofilin,[42] it is interesting to note that in both, brain and intestine, reelin initiates signaling cascades that affect the same cytosolic protein, cofilin, but we are far from knowing the cell signaling events triggered by reelin in the intestine.

The observations discussed so far reveal that the lack of reelin diminishes the rate of the crypt–villus unit renewal processes, but this intestinal response is opposite to that expected from the effects of the mutation on tissue architecture. Thus, the reelin-related expansion of the junctions might reflect a defective interaction of the cadherin ectodomain and the loss or reduction in E-cadherin function promotes intestinal cell proliferation, migration, and apo- ptosis[43,44] and reduces the number of Goblet cells.[44] And recent studies recognize a role for the desmosomes as sensors of environmental and cellular cues,[45] in tumor suppression[46] and in maintaining the shape and length of actin-rich mi- crovilli.[47] Regarding the latter role of demosomes, neither the length nor the number of microvilli are significantly modified by the reeler mutation. Reelin could overlap functionally with systems that either act identically or perform the same function, but in mechanistically distinct manners. Consequently, a component that is crucial under nonphysiological circumstances can be less relevant under physiological conditions, due to other compensating mechanisms. It is interesting to point out that the gastrointestinal tract, in addition to nutrient absorption, displays endocrine, immunologic, metabolic, and barrier functions and several observations suggest that reelin may protect the intestine from the development of pathologies. (1) The mutation reduces the number of Paneth cells. These cells secrete into the lumen of the crypts a number of antibacterial molecules in response to bacterial antigens, thereby contributing to the maintenance of gastrointestinal barrier.[3] They have also been implicated in the development of inflammatory bowel disease[48] and their location adjacent to stem cells suggests that they play a critical role in defending epithelial cell renewal.[3] (2) The wider extracellular space of the epithelial junctions may favor exposure to external pathogens. (3) The homeostasis of the intestinal epithelium is based on the balance between cell proliferation, differentiation, and apoptosis. The loss of control of these processes leads to cancer[49] and we have observed that reelin expression is decreased in human colon tumors.[50] (4) The absence of reelin reduces the intestinal expression of a large number of genes that code for proteins involved in the intestinal immune response, inflammation, and cancer processes.[17] As several reports have proposed a role for reelin in tissue repair in both, neural[31,51–53] and non- neural tissues,[32,51,54] its involvement in the activation of cell proliferation and migration during the mucosal regenerative response triggered by injury could not be discarded.

In conclusion, our work *in vivo* demonstrates for the first time that reelin controls crypt–villus unit homeostasis. The results also support the view that reelin may play a role in the protection of the intestine from pathologies and even in the intestinal repair processes. How reelin exerts its effects and

the role of the reelin signaling system in the intestinal physiology remains unknown.

Acknowledgments

This work was supported by a grant from the Junta de Andaluc´ıa (CTS 5884) and by a fellowship from the Spanish Ministerio de Educación y Ciencia (AP2007-04201) to MD Vázquez-Carretero. We thank Dr. O. Pintado from the Cen- tro de Producción y Experimentación Animal of University of Sevilla for his technical advice. Electronmicroscopy images were obtained in the Centro de Investigación, Tecnología e Innovación, Universidad de Sevilla and in the Departamento de Histología y Anatom´ıa patológica, Universidad de Navarra.

Disclosure Statement

No competing financial interests exist.

References

1. van der Flier, L.G., and Clevers, H. Stem cells, self-renewal, and differentiation in the intestinal epithelium. Annu Rev Physiol 71, 241, 2009.
2. Bullen, T.F., Forrest, S., Campbell, F., Dodson, A.R., Hersh- man, M.J., Pritchard, D.M., *et al.* Characterization of epi- thelial cell shedding from human small intestine. Lab Invest 86, 1052, 2006.
3. Porter, E.M., Bevins, C.L., Ghosh, D., and Ganz, T. The multifaceted Paneth cell. Cell Mol Life Sci 59, 156, 2002.
4. Potten, C.S. Epithelial cell growth and differentiation. II. Intestinal apoptosis. Am J Physiol 273, 253, 1997.
5. Gumbiner, B.M. Cell adhesion: the molecular basis of tissue architecture and morphogenesis. Cell 84, 345, 1996.
6. Powell, D.W., Pinchuk, I.V., Saada, J.I., Chen, X., and Mifflin, R.C. Mesenchymal cells of the intestinal lamina propria. Annu Rev Physiol 73, 213, 2011.
7. Giancotti, F.G., and Ruoslahti, E. Integrin signaling. Science 285, 1028, 1999.
8. Andoh, A., Bamba, S., Brittan, M., Fujiyama, Y., and Wright, N.A. Role of intestinal subepithelial myofibroblasts in inflammation and regenerative response in the gut. Pharmacol Ther 114, 94, 2007.
9. Garc´ıa-Miranda, P., Peral, M.J., and Ilundáin, A.A. Rat small intestine expresses the reelin-Dab1 signalling pathway. Exp Physiol 223, 451,

2010.
10. D'Arcangelo, G., Miao, G.G., Chen, S.C., Soares, H.D., Morgan, J.I., and Curran T. A protein related to extracellular matrix proteins deleted in the mouse mutant reeler. Nature 374, 719, 1995.
11. Ilundain, A.A., García-Miranda, P., Vázquez-Carretero, M.D., and Peral, M.J. Intestinal homeostasis in control and reeler mice. J Physiol Sci 59, 344, 2009.
12. Peral, M.J., García-Delgado, M., Calonge, M.L., Durán, J.M., De La Horra, M.C., Wallimann, T., *et al.* Human, rat and chicken small intestinal Na^+ - Cl^- -creatine transporter, functional, molecular characterization and localization. J Physiol 545, 133, 2002.
13. Wilson, T.H., and Wiseman, G. The use of sacs of everted small intestine for the study of the transference of substances from the mucosal to the serosal surface. J Physiol 123, 116, 1954.
14. Gown, A.M., and Willingham, M.C. Improved detection of apoptotic cells in archival paraffin sections, immunohisto- chemistry using antibodies to cleaved caspase 3. J Histochem Cytochem 50, 449, 2002.
15. Wang, L., Li, J., Li, Q., Zhang, J., and Duan, X.L. Morpho- logical changes of cell proliferation and apoptosis in rat je- junal mucosa at different ages. World J Gastroenterol 9, 2060, 2003.
16. Ramachandran, A., Madesh, M., and Balasubramanian, K.A. Apoptosis in the intestinal epithelium, its relevance in nor- mal and pathophysiological conditions. J Gastroenterol He- patol 15, 109, 2000.
17. García-Miranda, P., Vázquez-Carretero, M.D., Gutiérrez, G., and Ilundáin, A.A. Lack of reelin modifies the gene ex- pression in the small intestine of mice. J Physiol Biochem 68, 2015, 2012.
18. Hermiston, M.L., Wong, M.H., and Gordon, J.I. Forced ex- pression of E-cadherin in the mouse intestinal epithelium slows cell migration and provides evidence for nonautono- mous regulation of cell fate in a self-renewing system. Genes Dev 10, 985, 1996.
19. Zhang, A.H., Rao, J.N., Zou, T., Liu, L., Marasa, B.S., Xiao, L., *et al.* p53-dependent NDRG1 expression induces inhibi- tion of intestinal epithelial cell proliferation but not apo- ptosis after polyamine depletion. Am J Physiol Cell Physiol 293, 379, 2007.
20. Ghaleb, A.M., McConnell, B.B., Kaestner, K.H., and Yang, V.W. Altered intestinal epithelial homeostasis in mice with intestine-specific deletion of the Krüppel-like factor 4 gene. Dev Biol 15, 310, 2011.
21. Ose, T., Kadowaki, Y., Fukuhara, H., Kazumori, H., Ishihara, S., Udagawa, J., *et al.* Reg I-knockout mice reveal its role in regulation of cell

growth that is required in generation and maintenance of the villous structure of small intestine. On- cogene 26, 349, 2007.

22. Ramalho-Santos, M., Melton, D.A., and McMahon, A.P. Hedgehog signals regulate multiple aspects of gastrointes- tinal development. Development 127, 2763, 2000.
23. Pinto, D., Gregorieff, A., Begthel, H., and Clevers, H. Ca- nonical Wnt signals are essential for homeostasis of the in- testinal epithelium. Genes Dev 17, 1709, 2003.
24. Simmen, F.A., Xiao, R., Velarde, M.C., Nicholson, R.D., Bowman, M.T., Fujii-Kuriyama, Y., *et al.* Dysregulation of intestinal crypt cell proliferation and villus cell migration in

mice lacking Kruppel-like factor 9. Am J Physiol Gastrointest Liver Physiol 292, 1757, 2007.

25. Cattin, A.L., Le Beyec, J., Barreau, F., Saint-Just, S., Houllier, A., Gonzalez, F.J., *et al.* Hepatocyte nuclear factor 4alpha, a key factor for homeostasis, cell architecture, and barrier function of the adult intestinal epithelium. Mol Cell Biol 29, 6294, 2009.
26. Wang, Y., Shi, X., Qi, J., Li, X., Uray, K., and Guan, X. SIRT1 inhibits the mouse intestinal motility and epithelial prolifer- ation. Am J Physiol Gastrointest Liver Physiol 302, 207, 2012.
27. Vidrich, A., Buzan, J.M., Brodrick, B., Ilo, C., Bradley, L., Fendig, K.S., *et al.* Fibroblast growth factor receptor-3 regu- lates Paneth cell lineage allocation and accrual of epithelial stem cells during murine intestinal development. Am J Physiol Gastrointest Liver Physiol 297, 168, 2009.
28. Gumbiner, B.M. Regulation of cadherin mediated adhesion in morphogenesis. Nat Rev Mol Cell Biol 6, 621, 2005.
29. Kim, H.M., Qu, T., Kriho, V., Lacor, P., Smalheiser, N., Pappas, G.D., *et al.* Reelin function in neural stem cell bi- ology. Proc Natl Acad Sci U S A 19, 4020, 2002.
30. Hack, I., Bancila, M., Loulier, K., Carroll, P., and Cremer, H. Reelin is a detachment signal in tangential chain-migration during postnatal neurogenesis. Nat Neurosci 5, 939, 2002.
31. Massalini, S., Pellegatta, S., Pisati, F., Finocchiaro, G., Farace, M.G., and Ciafrè, S.A. Reelin affects chain-migration and differentiation of neural precursor cells. Mol Cell Neurosci 42, 341, 2009.
32. Rebustini, I.T., Hayashi, T., Reynolds, A.D., Dillard, M.L., Carpenter, E.M., and Hoffman, M.P. miR-200c regulates FGFR-dependent epithelial proliferation via Vldlr during submandibular gland branching morphogenesis. Develop- ment 139, 191, 2012.
33. Khialeeva, E., Lane, T.F., and Carpenter, E.M. Disruption of reelin

signaling alters mammary gland morphogenesis. De- velopment 138, 767, 2011.

34. Ohkubo, N., Vitek, M.P., Morishima, A., Suzuki, Y., Miki, T., Maeda, N., and Mitsuda, N. Reelin signals survival through Src-family kinases that inactivate BAD activity. J Neurochem 103, 820, 2007.
35. Ge, G., and Greenspan, D.S. Developmental roles of the BMP1/TLD metalloproteinases. Birth Defects Res C Embryo Today 78, 47, 2006.
36. Yeung, T.M., Chia, L.A., Kosinski, C.M., and Kuo, C.J. Regulation of self-renewal and differentiation by the intes- tinal stem cell niche. Cell Mol Life Sci 68, 2513, 2011.
37. Cariello, N.F., Romach, E.H., Colton, H.M., Ni, H., Yoon, L., Falls, J.G., *et al.* Gene expression profiling of the PPAR-alpha agonist ciprofibrate in the cynomolgus monkey liver. Toxicol Sci 88, 250, 2005.
38. Bryja, V., Gradl, D., Schambony, A., Arenas, E., and Schulte, G. Beta-arrestin is a necessary component of Wnt/beta- catenin signaling *in vitro* and *in vivo*. Proc Natl Acad Sci U S A 104, 6690, 2007.
39. Yamazaki, T., Masuda, J., Omori, T., Usui, R., Akiyama, H., and Maru, Y. EphA1 interacts with integrin-linked kinase and regulates cell morphology and motility. J Cell Sci 122, 243, 2009.
40. McConnell, B.B., and Vertino, P.M. TMS1/ASC, the cancer connection. Apoptosis 9, 5, 2004.
41. Lau, C., Lytle, C., Straus, D.S., and DeFea, K.A. Apical and basolateral pools of proteinase—activated receptor-2 direct distinct signaling events in the intestinal epithelium. Am J Physiol Cell Physiol 300, 113, 2011.
42. Chai, X., Fö rster, E., Zhao, S., Bock, H.H., and Frotscher, M. Reelin stabilizes the actin cytoskeleton of neuronal processes by inducing n-cofilin phosphorylation at serine3. J Neurosci 29, 288, 2009.
43. Fouquet, S., Lugo-Mart´ınez, V.H., Faussat, A.M., Renaud, F., Cardot, P., Chambaz, J., *et al.* Early loss of E-cadherin from cell-cell contacts is involved in the onset of Anoikis in en- terocytes. J Biol Chem 279, 43061, 2004.
44. Schneider, M.R., Dahlhoff, M., Horst, D., Hirschi, B., Trü lzsch, K., Mü ller-Hö cker, J., *et al.* A key role for E-cadherin in intestinal homeostasis and Paneth cell maturation. PLoS One 5, 14325, 2010.
45. Green, K.J., and Gaudry, C.A. Are desmosomes more than tethers for intermediate filaments? Nat Rev Mol Cell Biol 1, 208, 2000.
46. Dusek, R.L., and Attardi, L.D. Desmosomes, new perpetrators in tumour suppression. Nat Rev Cancer 11, 317, 2011.
47. Sumigray, K.D., and Lechler, T. Desmoplakin controls mi- crovilli length but not cell adhesion or keratin organization in the intestinal

epithelium. Mol Biol Cell 23, 792, 2012.

48. Beisner, J., Stange, E.F., and Wehkamp, J. Paneth cell function-implications in pediatric Crohn disease. Gut Microbes 2,47, 2011.
49. Hanahan, D., and Weinberg, R.A. The hallmarks of cancer. Cell 100, 57, 2000.
50. García-Miranda, P., Galindo-Galindo, A., Ilundáin, A.A., and Peral, M.J. Reelin mRNA expression is reduced in hu- man colorectal cancer. Genes Nutr 6, S77, 2012.
51. Pulido, J.S., Sugaya, I., Comstock, J., and Sugaya, K. Reelin expression is upregulated following ocular tissue injury. Graefes Arch Clin Exp Ophthalmol 245, 889, 2007.
52. Lorenzetto, E., Panteri, R., Marino, R., Keller, F., and Buffelli, M. Impaired nerve regeneration in reeler mice after periph- eral nerve injury. Eur J Neurosci 27, 12, 2008.
53. Courtès, S., Vernerey, J., Pujadas, L., Magalon, K., Cremer, H., Soriano, E., *et al.* Reelin controls progenitor cell migration in the healthy and pathological adult mouse brain. PLoS One 6, 20430, 2011.
54. Kobold, D., Grundmann, A., Piscaglia, F., Eisenbach, C., Neubauer, K., Steffgen, J., *et al.* Expression of reelin in he- patic stellate cells and during hepatic tissue repair, a novel marker for the differentiation of HSC from other liver myofibroblasts. J Hepatol 36, 607, 2002.

Table 1. Oligonucleotides Sequences Used For Reverese Transcription-Polymerase Chain Reaction Assays

Gene symbol (5¢-3¢)	*Accession no.*	*Sense (5¢-3¢)*	*Antisense*
Reelin	NM_011261	GGACTAAGAATGCTTATTTCC	GGAAGTAGAATTCATCCATCAG
Dab1	NM_010014	GACATCACAGATCATCGG	CTGGTACACAGATTGTTCAC
VldlR	NM_013703	GTGTACTTGAAGACCACTGAAGAG	GCTGGCTCTGTTACCATTC
ApoER2	NM_053073	GAATGAAGGCAGCCAGAT	GTTGTCGAAATTCATGCTC
b-actin	NM_007393	ACCCACACTGTGCCCATCTA	CGGAACCGCTCATTGCC

Oligonucleotides were chosen according to the cDNA sequences entered in GenBank and designed using PerlPrimer program v1.1.14.Dab1, Disabled-1; VldlR, very low-density lipoprotein receptor.

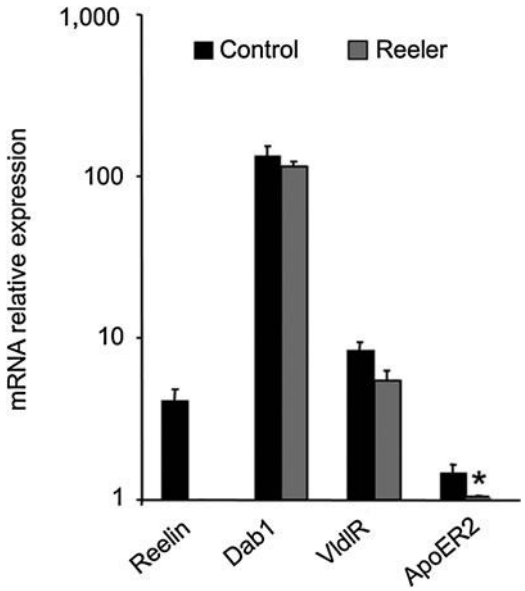

FIG. 1. Abundance of reelin, Disabled-1 (Dab1), apolipo- protein E receptor 2 (ApoER2) and very low-density lipo-protein receptor (VldlR) mRNAs in the small intestine of control and reeler mice. Reverse transcription-polymerase chain reaction was performed using total RNA isolated from the small intestine of 1-month-old mice. The values represent the means – SEM of relative units of mRNA abundance on a semilogarithmic scale. The ApoER2 mRNA abundance measured in the reeler mice was set at one. Three reeler and three control mice were used. Student's t-test: *$p < 0.05$ reeler versus control mice.

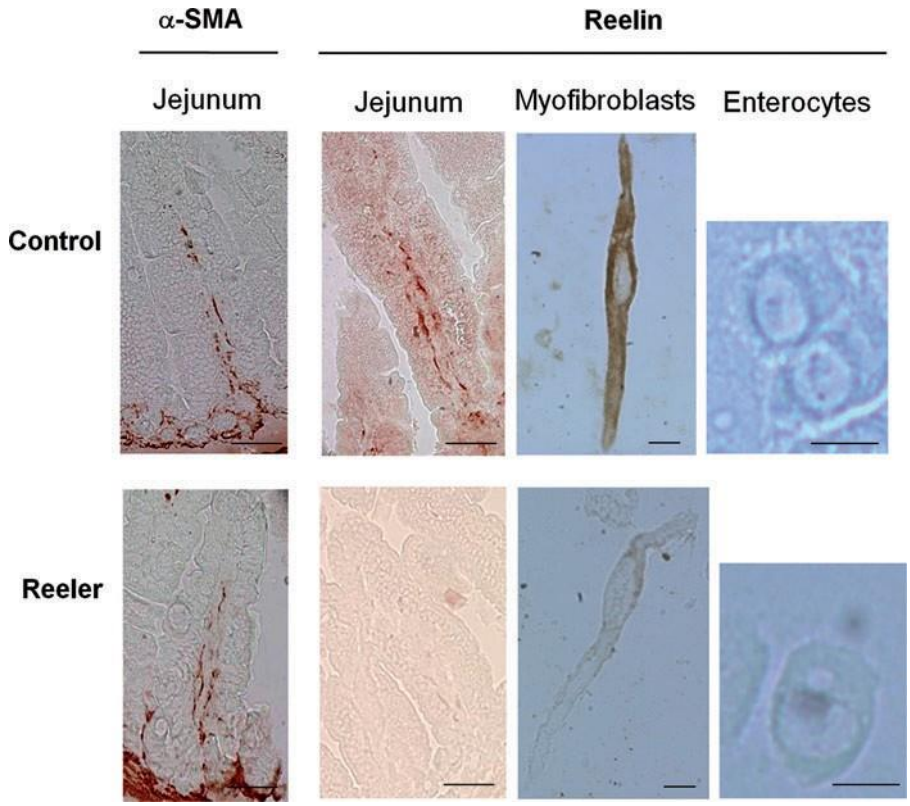

FIG. 2. Immunolocalization of a-smooth muscle actin (a-SMA) andreelin in the small intestine of control and reeler mice. Five micrometer paraffin sections of jejunum obtained from 15-day-old mice were incubated either with anti-a-SMA (1:200 dilution) or withanti-reelin (Calbiochem, 1:100 dilution) primary antibodies. Myofibroblasts and enterocytes obtained from 1-month-old mice were incubated with anti-reelin antibody (Santa Cruz, 1:50 dilution). Scale bars represent 50 mmin the intact tissue and 10 mm in theisolated cells. The photographs arerepresentative of three different assays performed on three reeler and three control mice.

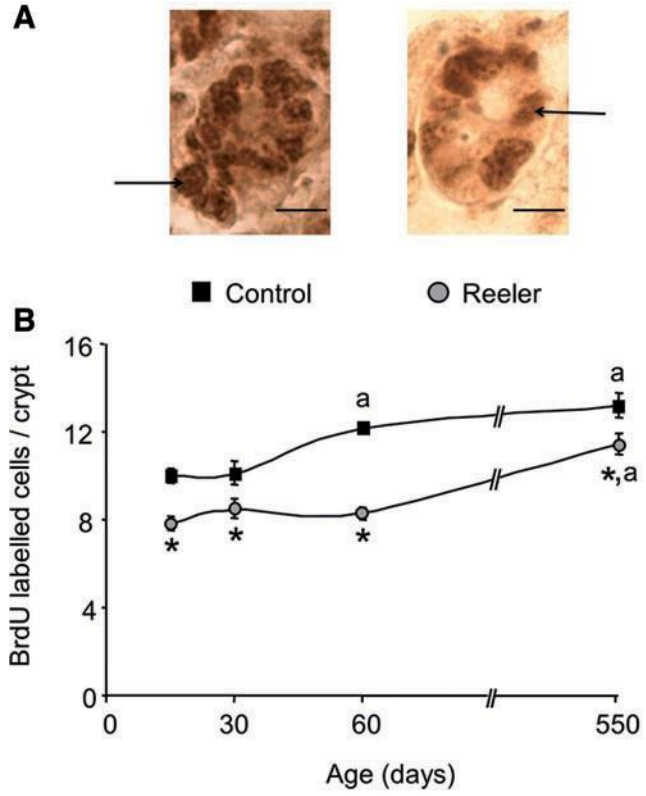

FIG. 3. Cell proliferation rate in the intestinal epithelium of control and reeler mice. Incorporation of 5-bromo deoxyur- idine (BrdU) into DNA was used as a marker of cell prolif- eration as described in Methods section. Fifteen- and 21-day-oldand 1-, 2-, 3-, and 18-month-old control and reeler mice were used. The number of cells labeled with a monoclonal anti- BrdU antibody (1:300 dilution) was determined by light microscopy in 30 crypts, well-oriented longitudinally, per mouse. (A) Representative sections of intestinal crypts. Ar- rows indicate BrdU-labeled cells. Scale bar represents 20 mm.

(C) Mean – SEM of the number of BrdU-labeled cells per crypt. The number of animals used per age was three reeler and three control mice. One-way ANOVA showed an effect of the mutation and of the maturation on cell proliferation($p < 0.001$). Newman-Keuls' test: $*p < 0.001$ reeler versus control mice, $^{a}p < 0.001$ versus 15-day-old mice.

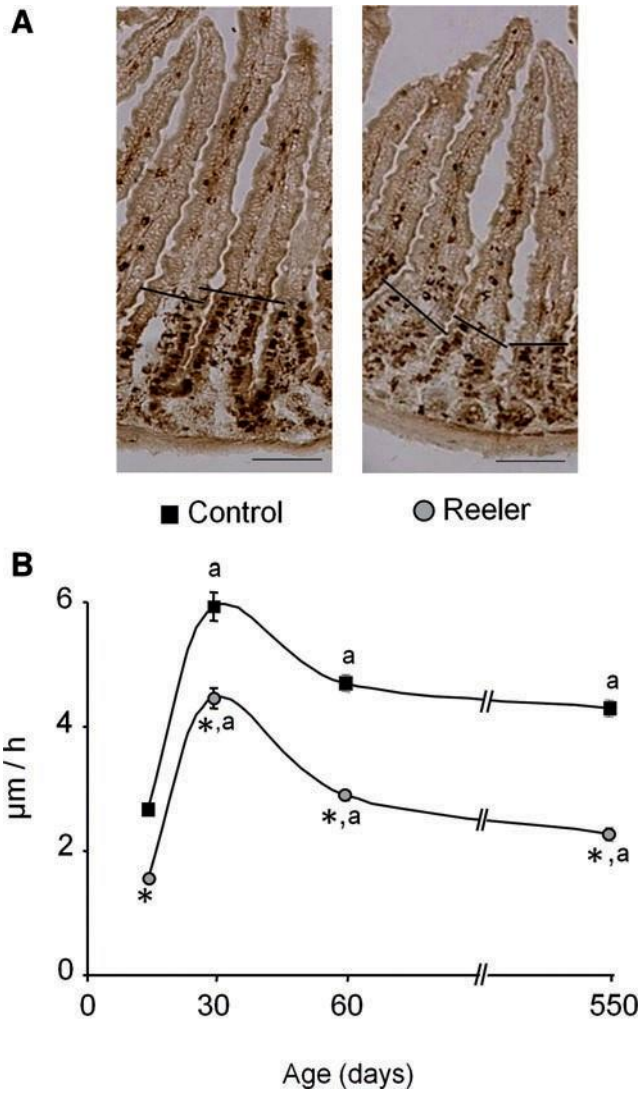

FIG. 4. Cell migration rate in the small intestine of control and reeler mice. Mice were injected with BrdU 32 h before death (see Methods section). The distance between the fore- most-labeled cells were measured and used to determine the cell migration rate. (A) Representative sections of mice in- testine. Lines indicate the front of labeled cells used for cal- culating the enterocyte migration rate. Scale bar represents 100 mm. (B) Means – SEM of the distance (in mm) migrated per hour. Others details as in Figure 3. One-way ANOVA showed an effect of the mutation and of the maturation on cell migration rate ($p < 0.001$). Newman-Keuls' test: *$p < 0.001$ reeler versus control mice, $^{a}p < 0.001$ versus 15-day-old mice.

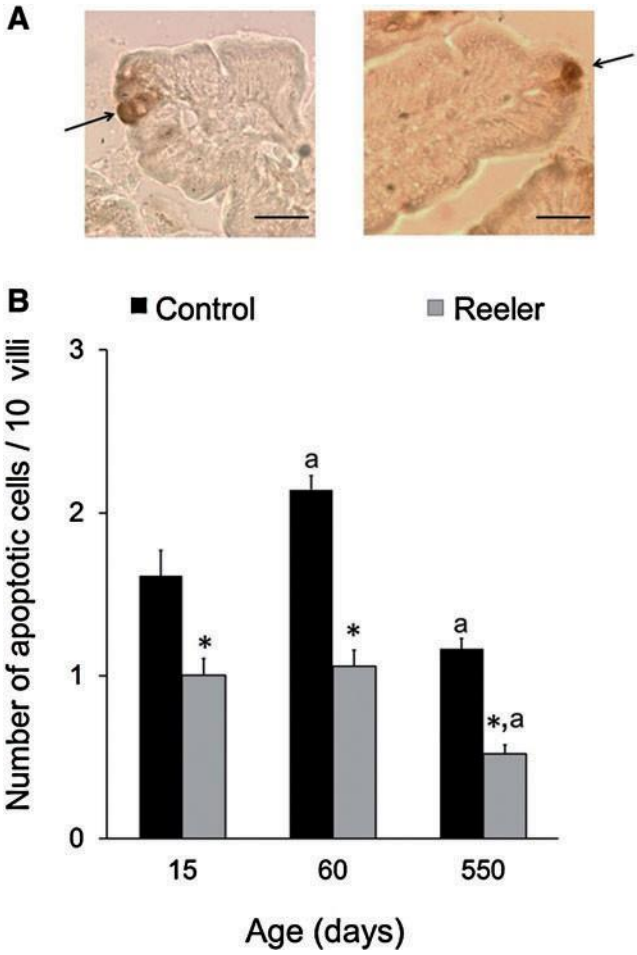

FIG. 5. Cell apoptosis in the small intestine of control and reeler mice. Sections of small intestine were incubated with anti-cleaved Caspase-3 antibody, 1:200 dilution, as described in Methods section. (A) Examples of apoptotic cells in the small intestine of control and reeler mice. Arrows indicate apoptotic cells. Scale bar represents 20 mm. (B) Means − SEM of the number of apoptotic cells per 10 villi. Others details as in Figure 3. One-way ANOVA showed an effect of the mutation and of the maturation on cell apoptosis ($p < 0.001$). Newman-Keuls' test: $^{*}p < 0.001$ reeler versus control mice, $^{a}p < 0.001$ versus 15-day-old mice. Color images available online at www.liebertpub.com/tea

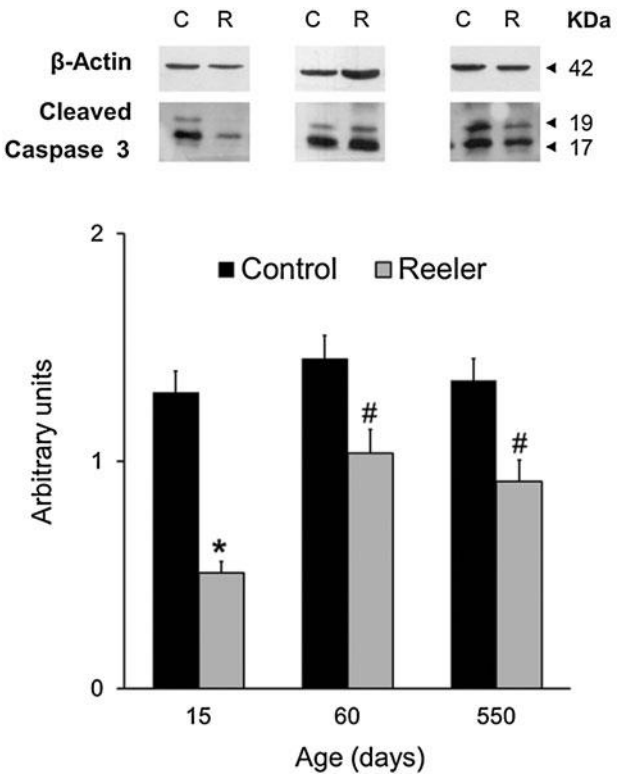

FIG. 6. Western blot analysis of intestinal cleaved Caspase-3 in control and reeler mice. Mice that were 0.5, 2, and 18 months old were used. 50 mg protein were loaded to each lane. The blots were probed with the polyclonal anti-cleaved Caspase-3 antibody, 1:1000 dilution, as described in the Methods section. Anti-b-actin antibody was used to normalize the bands. C, control; R, reeler. Histograms represent the means – SEM of the relative abundance of the 17-kDaband. One-way ANOVA showed an effect of the mutation on cell apoptosis ($p < 0.001$). Newman-Keuls' test: $^{*}p < 0.001$and $^{\#}p < 0.01$ reeler versus control mice.

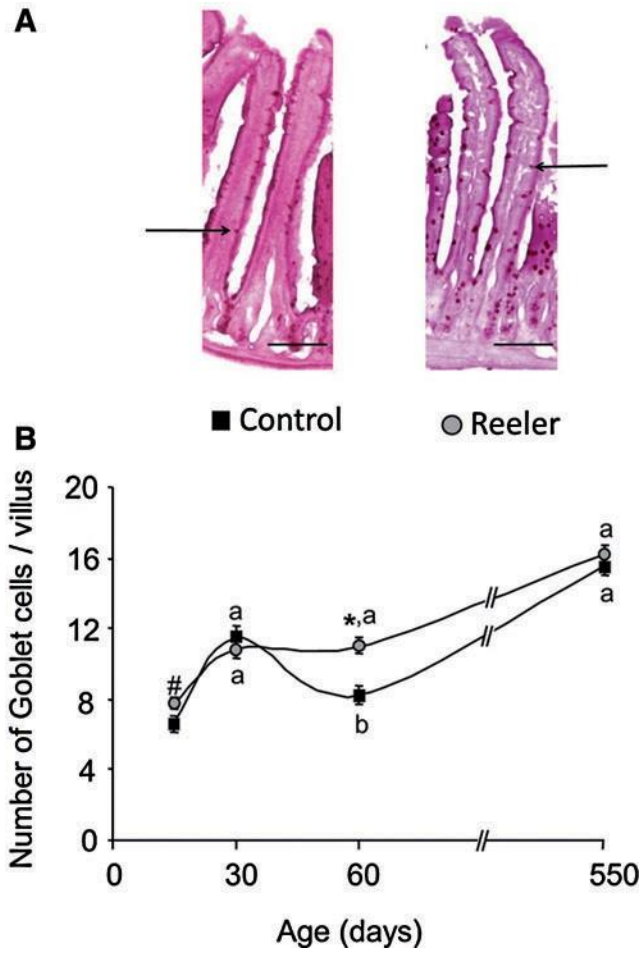

FIG. 7. Number of Goblet cells in the small intestine of control and reeler mice. Tissue was stained with Periodic Acid-Shiff Staining System. (A) Examples of Goblet cells in the intestine of control and reeler mice. Arrows indicate Goblet cells. Scale bar represents 100 mm. (B) Means – SEM of the number of Goblet cells per villus. Others details as in Figure 3. One-way ANOVA showed an effect of the mutation and of the maturation on the number of Goblet cells ($p < 0.001$). Newman-Keuls' test: $^{*}p < 0.001$ and $^{\#}p < 0.05$ reeler versus control mice, $^{a}p < 0.001$ and $^{b}p < 0.05$ versus 15-day-old mice.

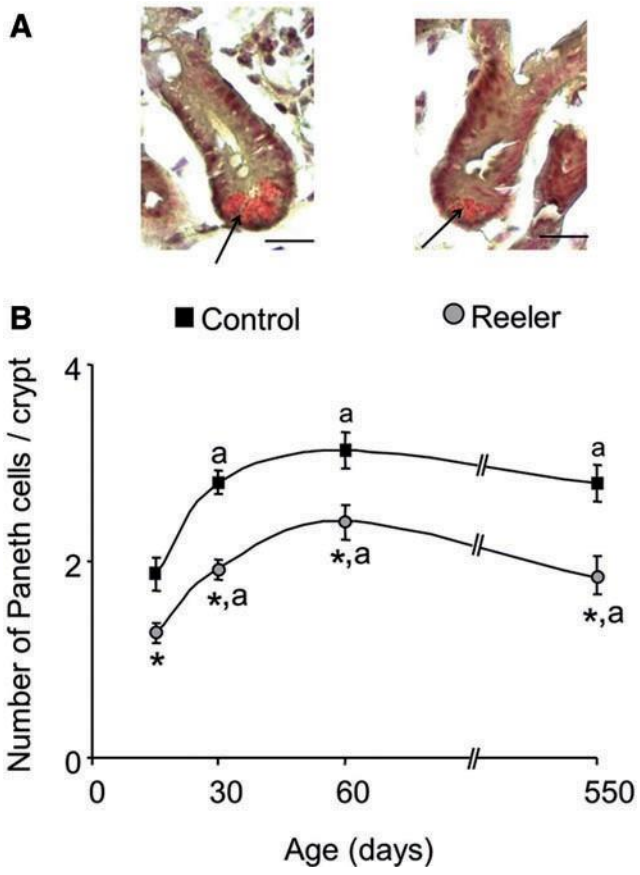

FIG. 8. Number of Paneth cells in the small intestine of control and reeler mice. Tissue was stained with phloxine- tartrazine as described in Methods section. (A) Examples of Paneth cells in the crypts of control and reeler mice. Arrowsindicate Paneth cells. Scale bar represents 20 mm. (B) Means – SEM of the number of Paneth cells per crypt. Others details as in Figure 3. One-way ANOVA showed an effect of the mutation and of the maturation on the number of Paneth cells ($p < 0.001$). Newman-Keuls' test: *$p < 0.001$ reeler versus control mice, $^{a}p < 0.001$ versus 15-day-old mice.

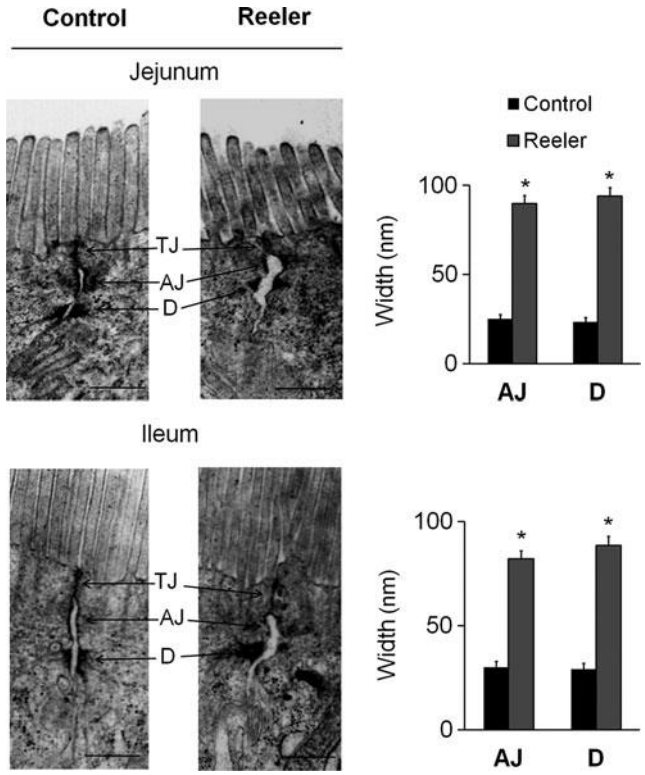

FIG. 9. Electron microscopic images of intestinal apical membrane domain of control and reeler mice. Microvilli and apical junctions of 1-month-old control and reeler mice are shown. Scale bar represents 500 nm. TJ, tight junctions; AJ, adherens junction; D, desmosome. The histogram represents the average width of the junctions (six to eight junctions were examined per type of mouse). The microphotographs are representative of three different assays performed on three reeler and three control mice. Student's t-test: *$p < 0.001$ reeler versus control mice.

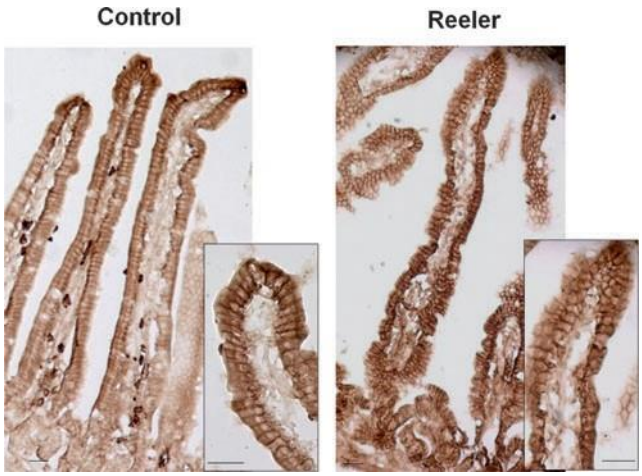

FIG. 10. Immunolocalization of E-cadherin in the intestinal epithelium of control and reeler mice. Ten micrometer cryo- sections of jejunum obtained from 1-month-old mice were incubated with the primary anti-E-cadherin antibody (1:500 dilution). The photographs are representative of three differ- ent assays performed on three reeler and three control mice.